Toward Improving Selectivity in Affinity Chromatography with PEGylated Affinity Ligands: The Performance of PEGylated Protein A

José González-Valdez
Centro de Biotecnología FEMSA, Tecnológico de Monterrey, Monterrey, NL 64849 México

Alex Yoshikawa and Justin Weinberg
Dept. of Chemical Engineering, Carnegie Mellon University, Pittsburgh, PA 15213

Jorge Benavides and Marco Rito-Palomares
Centro de Biotecnología FEMSA, Tecnológico de Monterrey, Monterrey, NL 64849 México

Todd M. Przybycien
Depts. of Biomedical Engineering and Chemical Engineering, Carnegie Mellon University, Pittsburgh, PA 15213

DOI 10.1002/btpr.1994
Published online October 18, 2014 in Wiley Online Library (wileyonlinelibrary.com)

Chemical modification of macromolecular affinity chromatography ligands with polyethylene glycol chains or "PEGylation" can potentially improve selectivity by sterically suppressing non-specific binding interactions without sacrificing binding capacity. For a commercial protein A affinity media and with yeast extract (YE) and fetal bovine serum (FBS) serving as mock contaminants, we found that the ligand accounted for more than 90% of the media-associated non-specific binding, demonstrating an opportunity for improvement. The IgG static binding affinity of protein A mono-PEGylated with 5.0 and 20.7 kDa poly(ethylene glycol) chains was found to be preserved using a biomolecular interaction screening platform. Similar in situ PEGylations of the commercial protein A media were conducted and the modified media was functionally characterized with IgG solutions spiked with YE and FBS. Ligand PEGylation reduced the mass of media-associated contaminants by a factor of two to three or more. Curiously, we also found an increase of up to 15% in the average recovery of IgG on elution after PEGylation. Combined, these effects produced an order of magnitude increase in the IgG selectivity on average when spiked with YE and a two- to three-fold increase when spiked with FBS relative to the commercial media. Dynamic binding capacity and mass-transfer resistance measurements revealed a reduction in dynamic capacity attributed to a decrease in IgG effective pore diffusivity and possibly slower IgG association kinetics for the PEGylated protein A ligands. Ligand PEGylation is a viable approach to improving selectivity in affinity chromatography with macromolecular ligands. © 2014 American Institute of Chemical Engineers *Biotechnol. Prog.*, 30:1364–1379, 2014
Keywords: bioseparations, affinity chromatography, PEGylation, protein A, antibody purification

Introduction

Affinity chromatography is a highly selective purification technique in common use in the downstream processing of recombinant proteins. For example, immobilized Staphylococcal protein A (SPA) media is central to "platform" processes for the purification of IgG-class monoclonal antibodies (mAbs).[1–3] In the case of SPA-based media for mAb purification, the specific binding of one of the five binding domains of SPA and the mAb constant Fc domain, as well as the heavy chain variable domain for the V_H3 subfamily, is exploited at neutral pH during column loading.[2,4] Unbound contaminants such as host cell proteins, host cell DNA, and virus particles are then removed by a series of washing steps, often at somewhat lower pH.[5] Ideally, the mAb is the only species left bound to the media at this point. Purified mAb is recovered in a subsequent elution step by dropping the solution pH to 3–4 to disrupt the binding interaction.[6] In reality, some non-specific contaminant binding occurs resulting in co-elution with the target and necessitating stringent cleaning steps. In mAb purification, contaminants may bind to both the SPA media and to the mAb itself, a phenomenon known as "hitchhiking."[5,7,8]

We aim to improve the selectivity of affinity chromatography media based on macromolecular ligands by depressing non-specific interactions between the ligand and contaminants. The selectivity, α, of an affinity media is given by

$$\alpha_{\text{target,cont}} = \frac{q_{\text{target}}}{q_{\text{cont}}} \frac{c_{\text{cont}}}{c_{\text{target}}} \tag{1}$$

where q_i and c_i represent the bound and free concentrations of target or contaminant, respectively. As selectivity increases, the

Correspondence concerning this article should be addressed to T. M. Przybycien at todd@andrew.cmu.edu.

purity of the eluted target increases, reducing the burden on and perhaps even the number of subsequent purification steps. It is possible to increase selectivity by using protein engineering to increase the binding affinity of the ligand for target, thereby enabling more stringent wash steps to be used to remove a greater portion of the contaminants. However the binding affinities of commercial media for target are already quite strong with equilibrium dissociation constants for mAbs with SPA media ranging from 0.2 μM to 2.0 μM.[9] Further increases in affinity will necessitate harsher elution conditions with the potential for degradation of both media and target.[10] By instead depressing the amount of bound contaminants, the stringency of the washing and cleaning steps may be decreased while maintaining the stringency of the elution step on par with that of the original media.

Here we test the hypothesis that ligand PEGylation, the covalent attachment of poly(ethylene glycol) (PEG) to the immobilized affinity ligand, will increase affinity media specificity by reducing non-specific contaminant binding. PEGylation provides a steric repulsion barrier for the core of the conjugate and has been widely used to impart *in vivo* "stealth" characteristics to pharmaceutical proteins.[11] A significant concern in this approach is the extent to which target dynamic binding capacity (DBC) can be preserved after ligand PEGylation. We were encouraged by the prior work of Wen and Niemeyer[12] who used ligand PEGylation with a variety of PEG species to improve the physical stability of an affinity media based on the labile ligand concanavalin A. They found that they could increase ligand stability toward thermal and organic solvent denaturation while maintaining up to 90% of the original static binding capacity of their media.

We found 2- to 3-fold reductions in non-specific protein binding for the PEGylated media and increased yields of target relative to the unmodified media resulting in order-of-magnitude increases in selectivity. Our model system comprised a commercial SPA media, with rabbit serum IgG and human plasma IgG as the targets and yeast extract (YE) and fetal bovine serum (FBS) as mock contaminants. We first verified that the immobilized SPA was responsible for the vast majority of media-associated non-specific protein adsorption via chromatographic retention studies. We then used a biosensor-based screening platform to probe the impact of conjugation with 5.0 kDa and 20.7 kDa PEG chains on the static binding affinity of the corresponding commercial SPA ligand. Finding the binding affinity largely preserved on PEGylation, we then conjugated the SPA media *in situ* with the same activated PEG species. We characterized the selectivity of the SPA columns before and after PEGylation via a standard load/wash/elute/regenerate chromatographic cycle with target spiked with varying concentrations of contaminants. Further characterization of the mass-transfer characteristics of the modified media revealed reductions in DBC that were attributed to increased pore mass-transfer resistance possibly and slower binding kinetics between IgG and the PEGylated protein A ligands.

Materials and Methods

Materials

Recombinant Staphylococcal Protein A (rSPA) and immobilized rSPA media were donated by RepliGen, Inc. (Waltham, MA). This particular rSPA contains 422 amino acids, has a molecular weight of 46.7 kDa, and consists of five wild type Fc binding domains (E, D, A, B, and C) together

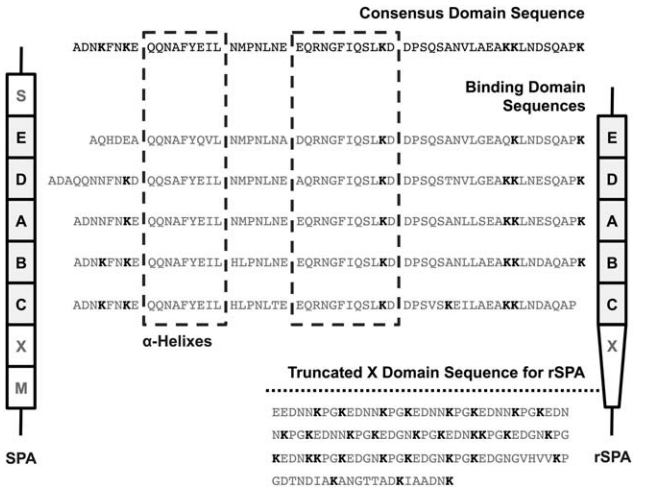

Figure 1. Comparative structures and amino acid sequences of wild type SPA and rSPA.

The approximate amino acid sequences of each of the IgG binding domains is presented showing the residues that form α-helix structures. The top sequence corresponds to the ancestral consensus for the homologous domains E, D, A, B, and C. The sequence for the truncated anchoring X domain of rSPA is shown at the bottom. Lysine (K) residues available for PEGylation are highlighted.

with a truncated form of the lysine-rich anchoring domain (X)[13]; the primary structure of rSPA, with the helical Fc binding domains highlighted, is shown in Figure 1. Immobilized rSPA media was provided as 5.0 mL pre-packed CaptivA PriMAB columns. The media have about 10 mg, or 0.21 μmol, of immobilized rSPA per mL of wetted resin per information provided by the manufacturer. The columns were 1.13 cm in diameter by 5 cm long and 1.2 cm in diameter by 4.4 cm long. The 1.13 cm × 5 cm columns were used in all experiments excepting the unmodified media controls in the media physical characterization work and the plate height work. Additionally, a 1.2 cm × 4.4 cm prepacked Sepharose 4FF column was provided by RepliGen as a control for physical characterization. Sepharose 4FF media (GE Healthcare, Piscataway, NJ), comprising 45–165 μm particles (90 μm mean particle diameter) of 4% crosslinked agarose, is the base matrix for the RepliGen media. A similar 5 mL column of unfunctionalized Sepharose CL-4B (GE Healthcare) was used to assess non-specific binding interactions with the Sepharose base matrix. The target species for the rSPA media was reagent grade rabbit serum IgG obtained from Sigma (Catalog No. I5006, St. Louis, MO). Mock contaminant species for spiking studies comprised YE from Fisher Scientific (Pittsburgh, PA) and Gibco FBS from Life Technologies Corp. (Grand Island, NY). Breakthrough and pulse experiments for column mass-transfer resistance characterization were performed with human IgG lyophilized from plasma obtained from Lee BioSolutions (Catalog No. 340-21, St. Louis, MO). Methoxy-PEG-propionaldehyde (mPEG-PA), with 5.0 kDa and 20.7 kDa molecular weights as determined by matrix-assisted laser desorption/ionization mass spectrometry, was donated by Dr. Reddy's Laboratories (Cambridge, United Kingdom). Dextrans, polyethylene glycols, and polyethylene oxides of various molecular weights used for inverse size exclusion chromatography (iSEC) experiments were obtained from Agilent Technologies (Santa Clara, CA), Amersham Biosciences (Piscataway, NY), Pharmacosmos (Holbaek, Denmark) and Sigma-Aldrich (St. Louis, MO). Phage lambda DNA used to characterize media

interstitial porosity was obtained from New England BioLabs (Ipswich, MA). All other PEGylation reaction buffer, chromatography buffer, and assay components were of reagent grade or better and obtained from Sigma–Aldrich (St. Louis, MO). All water was purified by reverse osmosis followed by treatment to 18 MΩ cm resistivity using a Barnstead NANOpure Diamond system from Barnstead International (Dubuque, IA).

Evaluation of the contribution of the rSPA ligand to non-specific binding

A standard SPA-based affinity chromatography mAb purification protocol suggested by RepliGen was used for *in situ* evaluations of non-specific contaminant binding interactions with the immobilized rSPA media as well as with the underivatized base matrix. For this set of experiments, a 5 mL column of Sepharose CL-4B was used as a stand-in for the Sepharose 4FF base matrix; Sepharose CL-4B media is also composed of 4% agarose particles ranging from 45 to 165 μm in diameter, but is not as highly cross-linked as 4FF. All chromatography was conducted with an Äkta Prime Plus system (GE Healthcare) maintained in a refrigerated room at 4°C. The columns were washed thoroughly with deionized water and equilibrated with a pH 7.0 phosphate buffered saline (PBS) buffer. Then, 0.5 mL of mock contaminant solution was injected. Contaminant solutions consisted of 0.33, 1.0, 3.0, 10, and 30 mg/mL solutions of YE or 1.0, 2.5, 5.0, 7.5, and 10.0% vol/vol solutions of FBS. A total of 6 column volumes of the pH 7.0 PBS buffer was used to load and then wash the columns. Elution was performed by switching to 10 column volumes of a pH 3.0, 100 mM glycine buffer with 50 mM NaCl. In this same step, the columns were stringently washed and regenerated. Afterwards, they were next re-equilibrated with 6 column volumes of the PBS buffer. The flow rate during the entire chromatographic process remained constant at 0.5 mL/min. The conductivity and the UV absorbance at 280 nm of the column effluent were monitored throughout. All experiments were performed in triplicate or more and the data is presented as the average of those results. Chromatographic data were analyzed using the PrimeView software that accompanies the Äkta Prime Plus chromatography system. Calibration of the UV absorbance with known concentrations of YE and FBS allowed conversion of observed chromatogram peak areas to contaminant masses for mass balance calculations. Comparison of the masses of contaminant in flow-through and retained peaks for the immobilized rSPA media and for the base matrix media allowed the relative contributions of the rSPA ligand and the base matrix to the observed non-specific binding interactions to be determined.

Preparation of free PEGylated rSPA

Before PEGylating the affinity chromatography media, we first tested our PEGylation approach on free ligand in solution to determine whether ligand structure and target binding functionality would be preserved after conjugation. The key decisions in PEGylation are the PEG molecular weight, the PEG structure (linear or branched), the coupling chemistry, and the conjugate polymer–protein molar ratio.[11] For protein drugs, effective PEG molecular weights have ranged from 5 kDa to 40 kDa.[14,15] Common, facile conjugation chemistries target protein free amino groups of lysine residues and N-terminus.[16] This was a concern for the RepliGen rSPA as it contains 55 lysine residues and one N-terminus[13,17]: as shown in Figure 1, the truncated X anchoring domain contains 30 lysine residues while the Fc binding domains, A through E, contain 25 lysine residues in total; importantly, one helical region in each binding site contains one lysine residue. To avoid widespread and indiscriminant PEGylation, we chose a reductive alkylation apporach based on linear, aldehyde-activated PEGs of 5.0 kDa and 20.7 kDa, and conducted the reaction at pH 5.1 to provide selectivity for the N-terminus.[18]

The conjugation procedure was modified from that reported by Cisneros-Ruiz et al.[19] For each conjugation reaction, 2.0 mL of an rSPA solution at 3.0 mg/mL in pH 5.1 and 100 mM phosphate buffer with 20 mM sodium cyanoborohydride were added to flasks containing 3.9 mg of 5.0 kDa or 15.4 mg of 20.7 kDa mPEG-PA; this gave a ~6:1 activated PEG:rSPA molar ratio. Each mixture was vigorously stirred for 17 h at 4°C with a magnetic stirrer and stored for further processing. Separation of modified and unmodified rSPA was performed using an Äkta Explorer 100 (GE Healthcare, Piscataway, NJ) chromatography system equipped with a HiPrep 16/60 column prepacked with Sephacryl S-300 High Resolution size exclusion chromatography (SEC) media (GE Healthcare). The mobile phase used for all size exclusion separations was a 10 mM sodium phosphate, pH 7.2 buffer with 150 mM potassium chloride at a flow rate of 0.5 mL/min; injected samples of 0.5 mL were processed in each run. Prior to SEC processing, the 5.0 kDa reaction mixture was subjected to an additional ultrafiltration step in 50 kDa nominal molecular weight cut-off Amicon Ultra-4 centrifugal filter units for 15 min at 4,000×*g*. Fractions corresponding to PEGylated rSPA species were pooled and concentrated to 1.0 mg/mL using 10.0 kDa nominal molecular weight cutoff Amicon Ultra-4 centrifugal filter units. Concentrations of rSPA were measured via UV absorbance at 280 nm in a Spectramax M2 microplate reader (Molecular Devices, CA); rSPA calibration curves gave an extinction coefficient of 0.0507 mL/(mg cm). All peak quantifications were made using the Äkta Explorer Unicorn Evaluation software.

The chromatograms obtained from the separation of the PEGylated rSPA species from each reaction mixture are shown in Figure 2. As noted, at least two peaks are obtained for the rSPA fractions processed from each reaction with earlier eluting peaks corresponding to higher molecular weight species. Figure 2A shows the chromatogram for the PEGylation reactions with 5.0 kDa mPEG-PA. The initial ultrafiltration step applied to these samples resulted in enrichment of the PEGylated material in the retentate and the enrichment of the unmodified species in the permeate; the retentate was retained for subsequent use. Figure 2B shows the chromatogram from the PEGylation reaction with 20.7 kDa mPEG-PA: SEC alone can discriminate between the generated conjugate and the unmodified rSPA; here, the first peak was recovered for subsequent use. PEGylated protein yields were 30.5 ± 1.1% and 67.1 ± 1.2% for the PEGylation reactions with 5.0 kDa and 20.7 kDa mPEG-PA, respectively, based on peak integration of replicate chromatograms; confidence limits here refer to the standard error. It was assumed that the majority of the PEGylated rSPA species produced were mono-PEGylated at the N-terminus as our prior experience with this reaction with several different proteins has shown.[19–21] Once sufficient purified PEG–rSPA

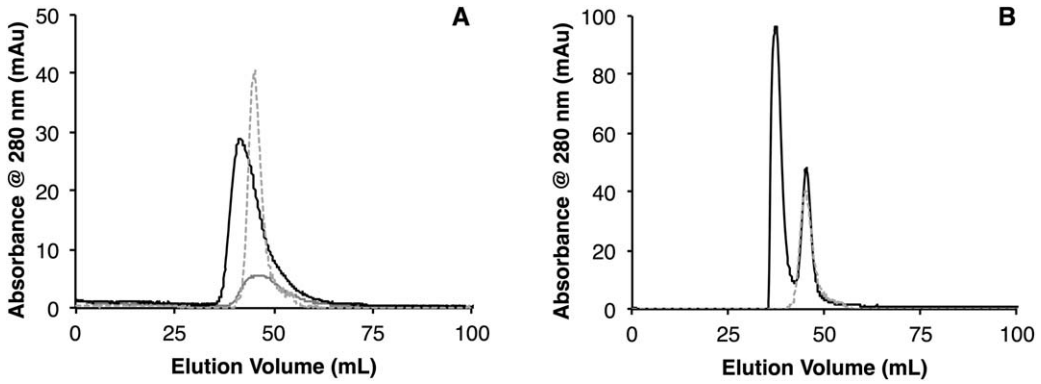

Figure 2. SEC chromatograms for the purification of rSPA species from PEGylation reaction mixtures.

Average chromatograms for the reactions with 5.0 kDa mPEG-PA (A) and 20.7 kDa mPEG-PA (B) are shown. Reaction mixtures for the 5.0 kDa mPEG-PA case (A) were ultrafiltered in 50.0 kDa MWCO filter units to generate streams that would aid their identification by SEC. The chromatograms for the retentate (■) and the filtrate (■) streams are shown. For each reaction mixture, the first peak in the elution profile corresponds to the PEGylated specie. The chromatogram for an unmodified rSPA standard at a concentration of 1.0 mg/mL is shown as a dashed line in both (A) and (B) for comparative purposes.

conjugate material was collected from the SEC fractions of the two reaction mixtures, the secondary structures and static IgG binding capacities of the conjugates were assessed and compared to that of the unmodified rSPA.

Structural and functional characterization of free PEGylated rSPA

Far-UV circular dichroism (CD) spectra were recorded using a Jasco J-810 spectropolarimeter (Easton, MD). Spectra were collected in the 190–240 nm wavelength range at room temperature using a quartz 1 cm path length cell. Samples of unmodified rSPA and the concentrated PEGylated species from each of the reactions were adjusted to obtain a final concentration of 1.25 μg/mL prior to analysis in pH 7.2, 20 mM phosphate buffer. In all spectral acquisitions, the scan speed was 100 nm/min, the bandwidth was 1 nm, and at least 10 scans were accumulated per spectrum. A protein-free background spectrum was recorded for each condition and subtracted from the protein spectra. The secondary structure contents of the protein samples were estimated with the CDPro software.[22]

IgG static binding kinetic assays of unmodified and conjugated rSPA were conducted to determine whether PEGylation adversely impacted function. Binding kinetics were assessed via a well-plate based optical interferometry technique using a FortéBio (Menlo Park, CA) Octet Red label-free biosensor platform after immobilization of the rSPA species on amine-reactive biosensor tips.[23] The following protocol was used. First, the sensor tips were hydrated in pH 5.0, 100 mM 2-(*N*-morpholino)ethanesulfonic acid (MES) buffer for 300 s. After hydration, the tips were transferred to wells that contained a 1:1 mixture of 0.1 M N-hydroxysuccinimide and 0.4 M 1-ethyl-3-(3-dimethylaminopropyl) carbodiimide solutions and were incubated for 300 s to activate the tips. Then the tips were transferred into wells which contained a 25.0 μg/mL solution of either unmodified or PEGylated rSPA in 10.0 mM PBS with 150 mM NaCl at pH 7.0. This protein immobilization step was conducted for 600 s. Two of the tips in each eight-tip run were not loaded with rSPA species to serve as controls. The remaining reactive groups were then quenched for 300 s in a 1.0 M, pH 8.5 ethanolamine buffer. After that, a baseline response was read with the same pH 7.0 PBS buffer for 600 s. Binding association and dissociation kinetics were then assessed by submerging the tips in 5, 10, or 15 mM solutions of rabbit serum IgG in PBS for 1,800 s under the same pH 7.0 PBS solution conditions. The tips were next transferred to wells that contained a pH 3.0, 100 mM glycine buffer with 50 mM NaCl, and incubated for 5,400 s to release the bound protein. The bind and release solution conditions were chosen to emulate chromatographic conditions recommended by RepliGen for use with CaptivA PriMAB chromatography columns. Tip washing was conducted in the same pH 3.0 dissociation buffer; a 600 s incubation time was used for this step. The baseline/bind/release/washing procedure was repeated. Binding kinetics in 100 mM glycine and 50 mM NaCl solutions with pH values adjusted to 4.0, 5.0, and 6.0 with NaOH were also tested in separate runs for each of the rSPA species to determine whether PEGylation altered the pH profile of the binding interaction. The experimental responses were fit to a 1:1 bimolecular interaction model with the built-in data analysis software provided by FortéBio to estimate the corresponding dissociation equilibrium constants.[24]

In situ preparation of immobilized PEGylated rSPA media

The rSPA affinity ligands in two CaptivA PriMab columns were PEGylated *in situ* with 5.0 and 20.7 kDa mPEG-PA using a similar approach to that for the free rSPA. Each column was installed and subjected to an initial wash with deionized water in an Äkta Prime Plus (GE Healthcare) chromatography system in a refrigerated room at 4°C. Then activated PEG solutions in reaction buffer were recirculated through the columns at a flow rate of 0.5 mL/min for 17 h. The solutions comprised 214 mg and 856 mg of 5.0 and 20.7 kDa mPEG-PA, respectively, diluted in 100 mL of a pH 5.1, 100 mM phosphate buffer with 20 mM sodium cyanoborohydride; this gave a ~40:1 activated PEG:rSPA ratio for the 5 mL columns. One milliliter samples of the recirculating solutions were taken each hour during the entire length of the conjugation reaction to track the extent of reaction via a PEG depletion assay. The assay for free PEG remaining in solution was based on the formation of a colored complex with barium chloride and iodine in solution.[25] Briefly, a 5.0% wt/vol $BaCl_2$ solution in 1.0 M HCl and a

1.3% wt/vol I_2 solution in deionized water were prepared. Calibration curves for optical absorbance were then made by taking 176 μL aliquots of 5.0 kDa or 20.7 kDa mPEG-PA solutions with known concentrations ranging from 1.0 to 45 μg/mL and mixing them with 44 μL of the $BaCl_2$ and 22 μL of the I_2 solutions in clear 96-well plates. After incubation for 15 min, absorbance was read at 535 nm in a Spectramax M2 microplate reader (Molecular Devices, Sunnyvale, CA). The samples obtained from the column PEGylation reactions were properly diluted and mixed in the same proportion to obtain residual mPEG-PA concentration values. These values were then used to calculate the PEGylation extent in the columns assuming that PEGylation was uniform throughout the media bed.

Evaluation of non-specific binding

One milligram per milliliter rabbit IgG samples spiked with YE or FBS contaminants were loaded onto columns containing PEG–rSPA or unmodified rSPA media and were subjected to the standard SPA-based affinity chromatography mAb purification protocol as described above. YE was added to the IgG samples to achieve final YE concentrations of 0.33, 1.0, 3.0, 10.0, and 30.0 mg/mL; similarly, FBS was added to achieve 1.0, 2.5, 5.0, 7.5, and 10.0% vol/vol concentrations. The conductivity and the UV absorbance at 280 nm of the column effluent were monitored throughout. All experiments were performed in triplicate or more and the data is presented as the average of those results with their corresponding standard errors. Chromatographic data were analyzed using the PrimeView software that accompanies the Äkta Prime Plus chromatography system. A UV detector calibration curve was prepared for IgG and, together with those prepared for YE and FBS, enabled observed peak areas to be reckoned in terms of species masses. Comparison of the masses of contaminant in flow-through and retained peaks for the PEGylated and unmodified rSPA media allowed the effectiveness of ligand PEGylation at reducing non-specific binding to be assessed.

Evaluation of dynamic binding capacity via breakthrough response

The DBC of the 20.7 kDa PEG–rSPA media was evaluated as a function of residence time via IgG breakthrough curves under binding conditions. Fronts of 2.0 mg/mL human polyclonal IgG were loaded onto the column in loading buffer for an extended period until ~80% breakthrough had been achieved as determined by bypassing the column; this was done to conserve protein. The flow rate was varied from 0.5 mL/min to 1.25 mL/min. The Äkta Prime Plus system was used for these experiments. Each experimental breakthrough curve had a small, early breakthrough due to the lack of retention of IgG_3 subclass species. The volume at 50% IgG_3 breakthrough was set as the void volume and the plateau absorbance after IgG_3 breakthrough, on the order of 5 mAU, was subtracted from each breakthrough curve.[9] The mass loaded per column bed volume at 10% breakthrough was used to determine the DBC.[26,27]

Physical characterization of media via inverse size exclusion chromatography

The interstitial porosities, ε, particle porosities, β, and effective average pore radii, r_{pore}, of the Sepharose 4FF, rSPA, 5.0 kDa PEG–rSPA, and 20.7 kDa PEG–rSPA media columns were characterized using iSEC. All iSEC experiments were performed on a Waters Alliance 2690 HPLC system (Milford, MA) with a Waters 2414 refractive index detector. iSEC experiments comprised sample injections of 100 μL pulses of 5 mg/mL glucose, dextrans, PEGs, and polyethylene oxides (PEOs) dissolved in pH 7.0 adjusted PBS and a mobile phase of the same buffer flowing at 1 mL/min. Viscosity concerns led us to prepare 1000 kDa and 1520 kDa polyethylene oxide samples at concentrations of 1 mg/mL and 0.4 mg/mL, respectively. Experiments were performed in triplicate. The molecular weight of the iSEC probes ranged from 180 Da to 1520 kDa. The retention volume of each sample was determined as the volume-based, baseline-corrected first statistical moment, μ_1, of the eluted peak. The experiments were repeated without a column in-line to enable subtraction of extra-column contributions to μ_1. The distribution coefficient, K_D, given by

$$K_D=(\mu_1/V_C-\ \varepsilon)/(1-\varepsilon) \tag{2}$$

was determined for each sample in each column, using the corresponding interstitial porosities and column volumes, V_C. The interstitial porosities were determined via separate injections of 100 μL of a 5 μg/mL solution of lambda DNA with the elution peak detected by UV absorbance at 260 nm with a Waters 996 PDA detector. Lambda DNA is linear and double stranded with a molecular weight of 31.5 MDa and is effectively excluded from all pores of these media, giving $K_{D,\lambda DNA}=0$. The particle porosity and effective average pore radius of each media were determined by fitting the partition coefficients of the probe species to a cylindrical pore model,[28]

$$K_D=\beta(1-r_{probe}/r_{pore})^2, \tag{3}$$

where r_{probe} is the viscosity radius of the probe; r_{probe} values were found for each probe species from established correlations with molecular weight for PEGs/PEOs and dextrans.[29] Glucose results were excluded from this analysis as it likely accesses micropores not accessible to proteins.[27] The estimates of β and r_{pore} were made via linear regressions of $\sqrt{K_D}$ vs. r_{probe}.

Evaluation of mass-transfer resistances via pulse response

Mass-transfer resistances were evaluated via IgG pulse response experiments performed under non-binding conditions with the Sepharose 4FF, rSPA, 5.0 kDa PEG–rSPA, and 20.7 kDa PEG–rSPA media columns. Each column was run in an isocratic mode in elution buffer[26] with injections of 100 μL pulses of 2.0 mg/mL human IgG. Experiments were performed in triplicate at flow rates of 0.75, 1.0, 1.25, 1.5, and 1.75 mL/min. These experiments were performed on the Waters Alliance 2690 system with a Waters 996 PDA detector set to measure absorbance at 280 nm. Peak moments were computed by fitting exponentially modified Gaussian (EMG) functions to the pulse responses in MATLAB using a Levenberg-Marquardt algorithm.[30,31] The EMG function fits were used to overcome inaccuracies in the direct numerical calculation of second moments by the moment method due to baseline noise[31]; EMG fits were judged to be good based on the match between fitted estimates and direct calculations of the zeroth and first moments

and the consistency of the fitted parameters from run to run. The parameter fitting uncertainty provided by the MATLAB "fit" routine was at least an order of magnitude smaller than the run-to-run variation in the fitted parameters. The fitted first moments and second central moments, μ_2, were corrected for extra-column contributions by subtraction of the corresponding moments determined without a column in-line. The corrected moments were used to compute the height equivalent to a theoretical plate, HETP, for each column and condition via[27]

$$\mathrm{HETP}=\frac{\mu_2' L}{\mu_1^2}. \tag{4}$$

where L is the column bed length.

The effective pore diffusivities, D_e, of IgG in the four media were then estimated from the corresponding van Deemter plots of the reduced plate height, $h=\mathrm{HETP}/d_p$, vs the reduced velocity, $v'=u_s d_p/D_o$, where d_p is the average media particle diameter, u_s is the superficial mobile phase velocity, and D_o is the bulk diffusivity of IgG, estimated to be $\sim 3.7 \times 10^{-7}$ cm^2/s.[32] A moment solution of the general rate model of chromatography for the case of non-binding conditions, and with mass-transfer resistances resulting from axial diffusion and dispersion, film diffusion and pore diffusion, provides the connection between the slope of the van Deemter plots and D_e.[27,33]

$$h=a+\frac{1}{30}\left(\frac{\varepsilon}{1-\varepsilon}\right)\left(\frac{\mu_1-\varepsilon V_C}{\mu_1}\right)^2\left(\frac{10}{Sh}+\frac{D_o}{D_e}\right)v' \tag{5}$$

where a is a constant approximating axial diffusion and dispersion contributions to h and Sh is the Sherwood number which expresses the dimensionless film mass-transfer coefficient. The Sherwood number was estimated from a correlation for mass transfer in packed beds[27,33]

$$Sh=\frac{1.09}{\varepsilon}Re_p^{0.33}Sc^{0.33} \tag{6}$$

here Re_p is the particle Reynolds number and Sc is the Schmidt number.

Results and Discussion

Significance of immobilized rSPA in non-specific retention of contaminants

The role of the immobilized rSPA ligand relative to the base matrix in the non-specific retention of contaminants was determined by comparing chromatograms for YE processed with rSPA media and un-functionalized Sepharose CL-4B media, both using the standard mAb affinity chromatography protocol. The resulting chromatograms are compared in Figure 3; note that the UV detector output is shown on a logarithmic scale on the first y-axis. The measured mobile phase conductivity is also shown in Figure 3 on the second y-axis to provide landmarks for the progression through the sequence of load/wash, elution/regeneration, and re-equilibration step gradients. The load/wash step employs pH 7.0 PBS buffer and the conductivity has a value of around 14 mS/cm. Next, the pH is lowered using pH 3.0 glycine buffer with 50.0 mM NaCl, resulting in a conductivity of about 6 mS/cm, to elute and recover the target protein and is maintained for several column volumes to regenerate the resin. Finally the column is re-equilibrated with the load/wash buffer, returning the conductivity to its original value, and completing the chromatographic run.

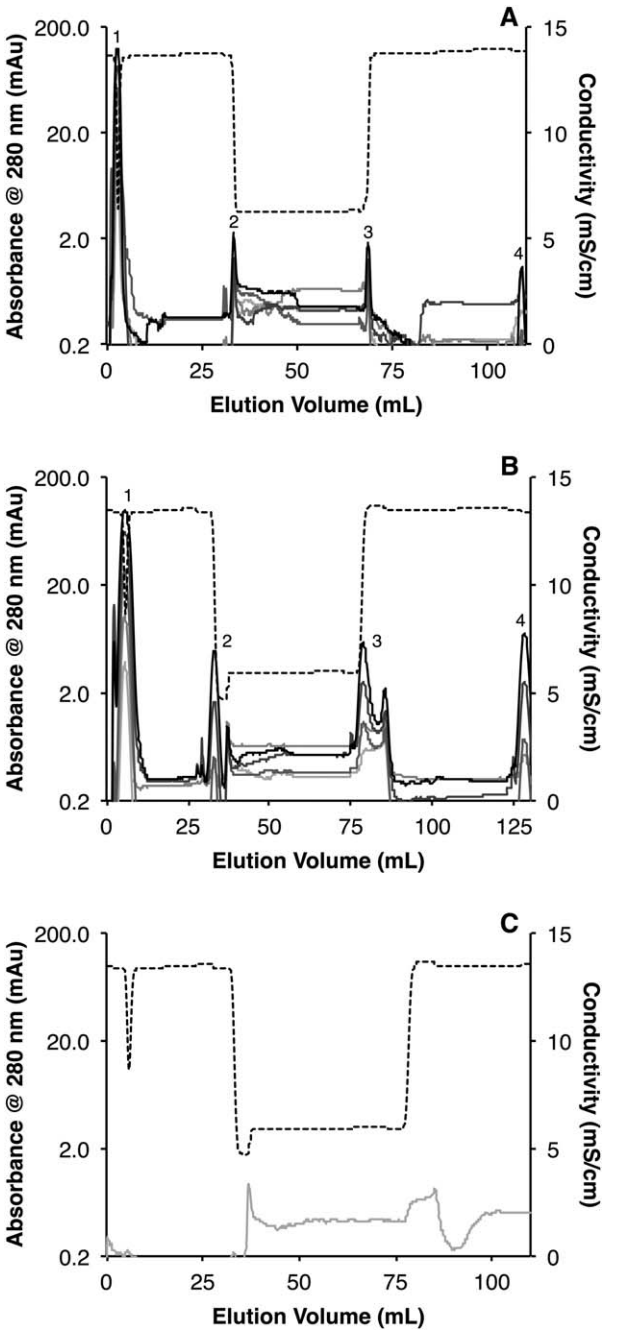

Figure 3. Average chromatographic elution profiles of YE on (A) unfunctionalized Sepharose CL-4B and (B) unmodified rSPA media columns.

The average buffer background signal from the detector for the unmodified rSPA AC column is shown in (C). Tested YE samples had concentrations of ■ 0.33, ■ 1.0, ■ 3.0, ■ 10.0, and ■ 30.0 mg/mL. Note that the lefthand axis shows UV absorbance at 280 nm on a logarithmic scale to emphasize the retained contaminant peaks and the peak groups have been labeled as 1, 2, 3, and 4 as described in the text. The conductivity profile (dashed line) corresponds to the righthand axis and is shown to provide landmarks for the standard mAb purification step gradients employed for SPA-based chromatography. The initial high conductivity corresponds to the load and wash steps; the step to low conductivity represents the elution step; the next step back to high conductivity represents the regeneration and re-equilibration steps.

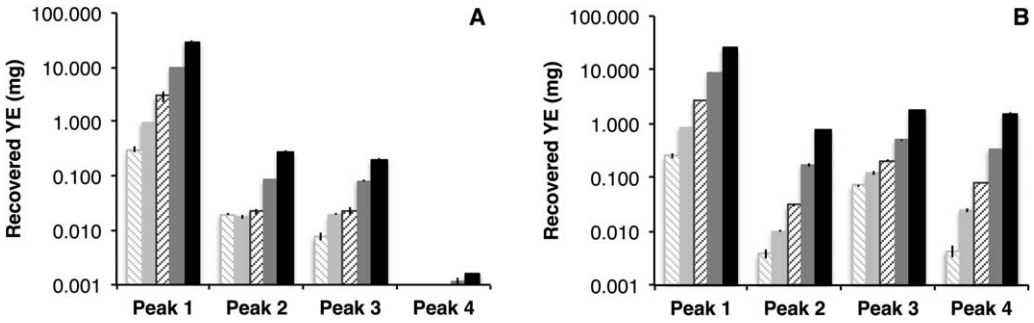

Figure 4. YE recoveries computed by integration of contaminant peaks 1 through 4 from Figure 3.

A: Shows results for a control column packed with unfunctionalized Sepharose CL-4B, and (B) shows results for the commercial, unmodified rSPA media column. Bars represent YE sample concentrations: 0.33 (▒, striped), 1.0 (▒), 3.0 (■, striped), 10.0 (▒), and 30.0 (■) mg/mL. The error bars represent the standard error of the mean of triplicate chromatographic experiments.

The chromatograms for the base matrix control column contain four groups of peaks: first, a large, non-retained peak of YE that elutes at roughly 5.0 mL corresponding to the void volume of the column; second, a peak at about 33.0 mL on the switchover to the elution/regeneration buffer; third, a peak at about 78.0 mL on the switch back for re-equilibration in the load/wash buffer; and fourth, a peak at about 110.0. The second, third, and fourth retained peaks are 1.5–2 orders of magnitude smaller than the first flow-through peak, as expected for a well-designed base matrix. These three small retained peaks represent the residual non-specific binding of contaminant species to the base matrix and are the peaks of interest here; a logarithmic scale is used for the UV-absorbance to emphasize these peaks. The areas and heights of these small peaks scale with the YE concentration loaded, indicating that these are indeed due to contaminant rather than to refractive index gradients or flow cell responses to pressure fluctuations at mobile phase changeovers. Given the resolution of the detector, the background signals due to the different buffers are used as shown in Figure 3 and the averaging of triplicate chromatograms, the absorbance data are significant down to about 0.5–1.0 mAu. Figure 4A reports the quantitation of the mass of material represented by each peak group in the base matrix control column experiments as a function of injected YE concentration using the YE calibration curve for the UV detector. This quantitation assumes that the resolved YE fractions within each peak have the same average extinction coefficient as the starting YE used for calibration. Adding up the masses of YE in each retained peak for a given YE concentration and comparing to the amount of YE injected at that concentration showed that $1.59 \pm 0.05\%$, $1.68 \pm 0.01\%$, $1.52 \pm 0.01\%$, $3.75 \pm 0.01\%$, and $9.16 \pm 0.01\%$ of the loaded YE mass became bound contaminant for the 0.3, 1.0, 3.0, 10, and 30 mg/mL YE injections, respectively; all results reported in this manner here and below represent the standard error of the mean of triplicate determinations unless otherwise stated.

Similar chromatograms are shown in Figure 3B for the rSPA column. Note that the non-retained YE peaks from the rSPA column are smaller, containing less material, than the corresponding non-retained peaks from the matrix control column. The second and third YE peaks occur at the buffer changeovers, as for the base matrix control column, but are larger with the third peak becoming a much larger doublet. There is also a fourth peak that occurs later in the re-equilibration. The second peak on the rSPA media represents contaminant species that may co-elute with a mAb product and the third and fourth peaks represent contaminants that must be removed prior to the re-use of the column. As for the base matrix control chromatograms, the YE peaks in the rSPA chromatograms were quantitated with the results shown in Figure 4B. In experiments with this column, adding up the masses of YE in each retained peak for a given YE concentration showed that the percentage of contaminant retained ranged between 10% and 15% averaging $12.5 \pm 4.3\%$ across the same 0.3–30 mg/mL YE concentration range. Plots of the amounts of YE bound to the base matrix control column and to the rSPA column are shown in Figure 5A along with the ratios of bound protein between both columns. It can be seen that as contaminant concentration increases so does the amount of bound contaminant.

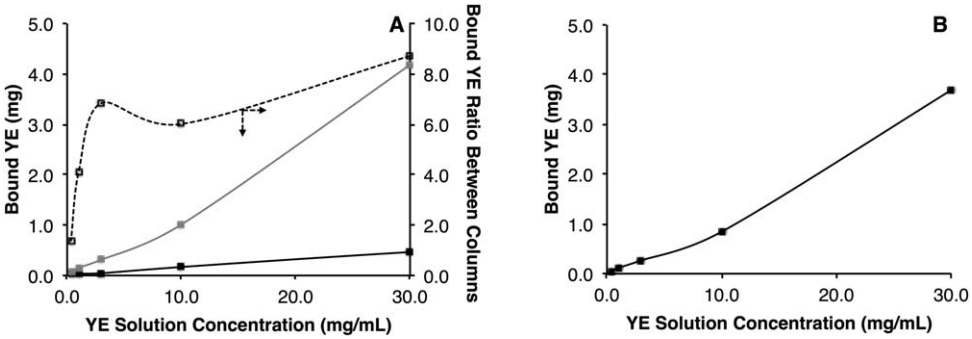

Figure 5. Comparison of YE binding at concentrations of 0.33, 1.0, 3.0, 10.0, and 30.0 mg/mL between columns.

A: The amount of bound YE in the Sepharose CL-4B column (■) is compared to that bound in an unmodified rSPA AC column (▒). The proportion between bound materials in both columns is also shown (□). B: Adsorption isotherm of YE on immobilized rSPA.

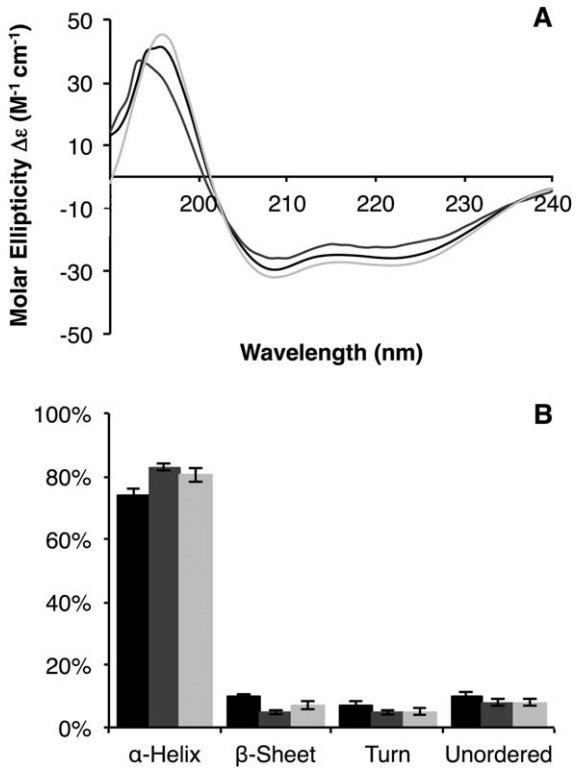

Figure 6. Secondary structure analysis of the purified PEGylated rSPA species.

The 5.0 kDa mPEG-PA and 20.7 kDa mPEG-PA PEGylated species are compared with native rSPA. A: Far-UV CD spectra of unmodified rSPA (black), 5.0 kDa PEG-rSPA conjugate (dark gray) and 20.7 kDa PEG-rSPA conjugate (light gray) plotted as molar ellipticity vs. wavelength. B: Secondary structure content estimates of native rSPA and the PEGylated rSPA species obtained using CD Pro software; bar shading corresponds to line shading in Figure 6A. The error bars represent the standard error of the mean of triplicate experiments.

Comparing the total amount of non-specifically bound YE in peaks 2, 3, and 4 between the base matrix and rSPA media cases, the rSPA media has ~1.4–8.7 times more non-specific binding than the base matrix for at the YE spike concentration increases from 0.3–30 mg/mL YE injections, respectively. Thus it is clear that it is the rSPA grafted to the chromatographic support matrix that is responsible for retaining a significant portion of the contaminant YE species through the different steps of the chromatographic protocol. The isotherm for YE on immobilized rSPA, generated by the difference between the amounts of bound contaminant between the base matrix support column and the rSPA column, is shown in Figure 5B. These results suggest that chromatographic selectivity may be increased if a steric barrier to non-specific binding can be established by PEGylating the immobilized ligand without substantially decreasing target static or DBC. In turn, we would expect the purity of the eluted target to increase and that the wash, regeneration, and re-equilibration steps may be shortened and/or reduced in stringency.

Free PEG–rSPA conjugate structural and functional characterization

The structural impact of rSPA PEGylation was assessed via far-UV CD. The CD spectra of the PEG–rSPA conjugates from each reaction were similar to those of the unmodified protein as shown in Figure 6A and were also similar to those reported in literature for SPA.[34,35] The estimated secondary structure contents among the tested species, shown in Figure 6B, are also in good agreement with the expected highly-helical structure reported for SPA.[36] On close examination, a slight increase in the α-helical content is evident for the conjugates when compared to the unmodified protein. This may be significant since the helical regions in the A through E domains are responsible of IgG binding[37,38] and a slight change in structure may impact the binding kinetics and equilibrium.

The effects of PEGylation upon the static binding behavior of rSPA for IgG were next determined to assess whether our initial PEGylation approach would result in a chromatographically viable affinity ligand. Dissociation equilibrium constants, K_d's, were measured using an optical interferometry-based biosensor platform. We used the standard loading pH 7.0 PBS and elution pH 3.0 glycine buffers specified in the protein A column purification protocol to emulate chromatographic conditions. The pH profile of the IgG binding behavior was also determined using solutions with pH values adjusted between 4.0 and 6.0. Figure 7 presents the K_d values estimated from those experiments. For both of the conjugates and for unmodified rSPA, K_d ranged between 4.3 and 4.8 $\times$ 10^{-6} M for the pH 3.0 elution buffer. This is consistent with other reports of K_d for SPA and free human and rabbit IgG at pH 3.0 that range from 5 $\times$ 10^{-6} to 2.5 $\times$ 10^{-5} M.[9,36] Importantly, as pH is increased, K_d values decrease commensurate with the expected stronger binding affinity at neutral pH. The estimated K_d values for the unmodified rSPA and the 5.0 kDa PEGylated rSPA at pH 7 are about a factor of two larger than those reported by Hahn et al.[26] for several different commercial protein A media, indicating somewhat lower binding affinity; the K_d value for the 20.7 kDa polymer conjugate is about a factor of three larger. These data suggest that it is possible to PEGylate rSPA, in solution in this case, without eliminating its ability to bind IgGs at neutral pH and release them at acidic pH.

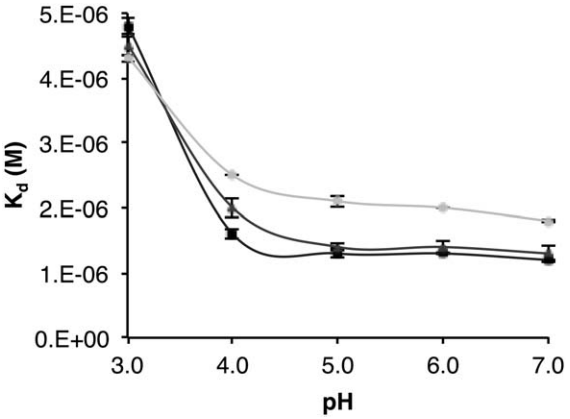

Figure 7. Dissociation equilibrium constant, K_d, for binding interactions between rSPA and the generated PEGylated conjugates with IgG as a function of pH.

K_d values for rSPA PEGylated species with 5.0 kDa mPEG-PA (dark gray line) and for species PEGylated with 20.7 kDa mPEG-PA (light gray line) are compared with those of unmodified rSPA (black line). The error bars represent the standard error of the mean of triplicate experiments.

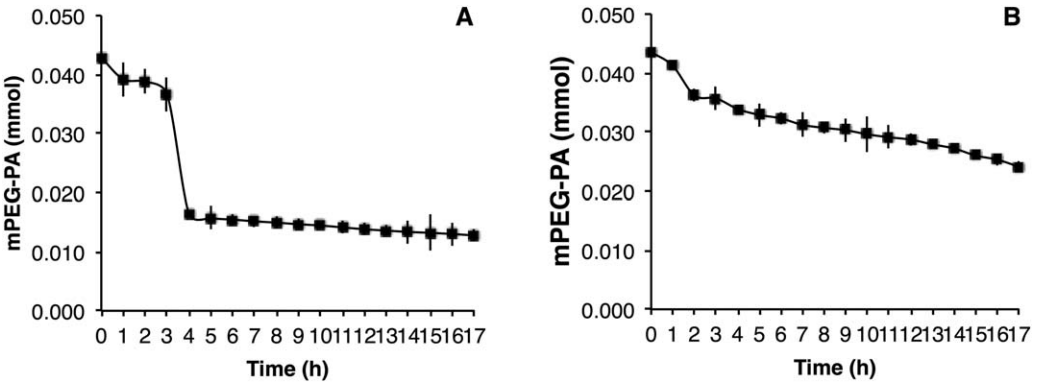

Figure 8. Decrease of activated PEG concentration in the recirculating PEGylation reaction buffers employed in the *in situ* modification of 5.0 mL rSPA affinity chromatography columns using: (A) 5.0 kDa mPEG-PA and (B) 20.7 kDa mPEG-PA.

The error bars represent the standard error of the mean of triplicate measurements.

Immobilized rSPA media in situ PEGylation

Two rSPA media columns were used for *in situ* ligand PEGylation with 5.0 and 20.7 kDa mPEG-PA by recirculating the activated PEGs in the reaction buffer as described previously. As expected, the assayed free PEG concentration decreased as the reaction progressed, as shown in Figure 8. It should be noted that the reductive alkylation chemistry used with the mPEG-PA reagents was not expected to modify the crosslinked agarose support matrix.

In the reaction with 5.0 kDa mPEG-PA, a dramatic increase in the extent of PEGylation is observed between hours 3 and 4 as indicated by the reduction in free polymer concentration. From then on, the decrease in the concentration of polymer decelerates. In the case of the column PEGylated with 20.7 kDa mPEG, the reaction starts rapidly in the first two hours and then decelerates. The percent modification was calculated using the known immobilized ligand concentration assuming that only ligand N-termini were reactive and that all immobilized ligands were equally reactive. After 17 h of reaction, total modifications of $75.0 \pm 0.9\%$ and $90.1 \pm 4.3\%$ for the columns PEGylated with 5.0 and 20.7 kDa mPEG-PA were achieved, respectively. Even though the reaction conditions were exactly the same for both cases, there were differences in the profiles and extents of modification achieved in the columns. This was surprising as the iSEC data shown further below indicates that, based on molecular size, both the 5.0 kDa and 20.7 kDa mPEG-PA should partition nearly completely into the media pores. After both *in situ* PEGylation reactions were terminated, the columns were flushed with re-equilibration buffer and used for chromatographic performance evaluation without further modification.

PEG–rSPA media functional characterization

Column performance was evaluated using 1.0 mg/mL samples of rabbit IgG spiked with different concentrations of YE or FBS, each serving as mock contaminants, and processed using the standard rSPA affinity chromatography protocol as described previously. Column performance for both columns was evaluated before and after PEGylation. Figure 9 presents the average chromatograms obtained from each of these runs in each of the columns tested. The IgG was consistently recovered in each run in a peak with an elution volume of about 37.0 mL during the elution step. For the IgG–YE mixtures, as before, four different contaminant peaks corresponding to the bind/wash (Peak 1), elution/regeneration (Peaks 2 and 3) and re-equilibration (Peak 4) steps were observed at elution volumes of ~5.0, 33.0, 78.0, and 125.0 mL. The IgG–FBS mixtures had a similar pattern of four peaks, but with significantly less contaminant binding than the IgG–YE mixtures. The main FBS contaminant peak was the flow-through peak of the bind/wash step at approximately 4.0 mL. The remaining peaks in the IgG–FBS mixtures occurred in a cluster around the switch from elution/regeneration to re-equilibration and were quantified together by mass balance to simplify calculations.

In general, PEGylation had no effect on the elution volume of contaminant or IgG peaks, but did result in a small increase in the size of the contaminant flow-through peaks and corresponding decreases in the size of the various retained contaminant peaks. These peak size effects were quantified by integrating each contaminant peak and applying the YE and FBS detector calibration curves. The results of these quantitative analyses are reported in Figure 10. From Figures 9 and 10, it can be seen that the vast majority of the contaminant protein exits in the flow-through in all cases, as expected for a well-designed media. However, there was a consistent small increase in the amount of YE and FBS contaminant exiting in the flow-through for the PEGylated media, indicative of a reduction in the amount of non-specific binding of contaminant species. For the YE spiking studies, this reduction in non-specific binding amount was distributed over the three retained contaminant peaks. The reductions in contaminant amounts in the various retained peaks ranged from a factor of two to negligible amounts, depending on conditions, with generally greater reductions seen at the lower spiked YE concentrations. For the FBS spiking studies, the lumped non-specific binding amount decreased uniformly. In this case, the amount of FBS contaminant binding decreased by factors ranging from two to one hundred. While the performances of the 5.0 kDa PEGylated and 20.7 kDa PEGylated columns were similar and were attributed to steric repulsions between contaminant species and the PEG chains attached to the immobilized rSPA, the 20.7 kDa PEGylated column tended to have less non-specific binding than the 5.0 kDa PEGylated column. Considering the greater molecular mass and extent of PEGylation and the corresponding increased excluded volume of the 20.7 kDa PEG media vs. the 5.0 kDa PEG media, this result makes sense.

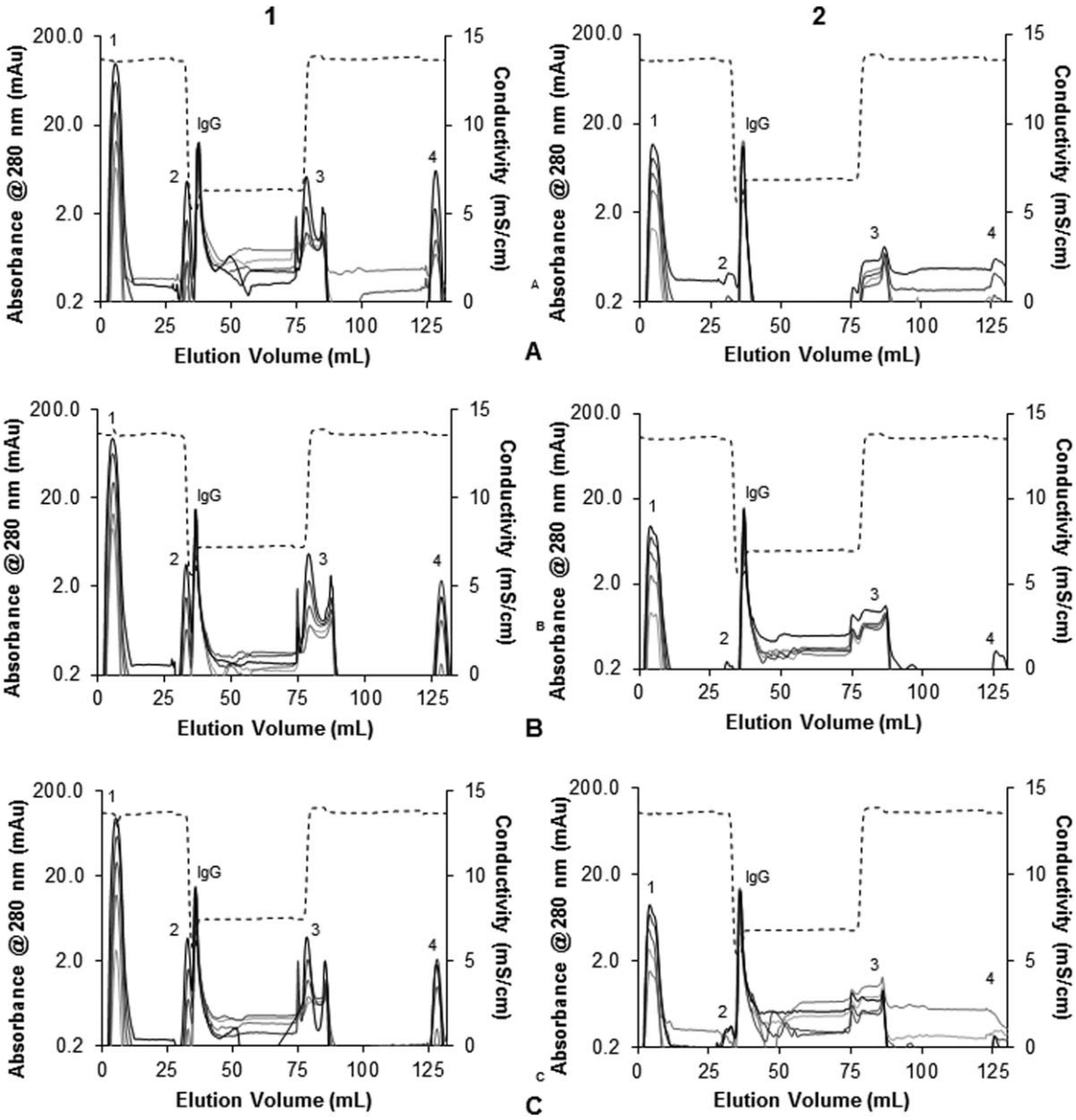

Figure 9. Comparison of the average chromatograms of 1.0 mg/mL rabbit IgG samples spiked with YE (Column 1; ■ 0.33 mg/mL, ■ 1.0 mg/mL, ■ 3.0 mg/mL, ■ 10.0 mg/mL, ■ 30.0 mg/mL) and FBS (Column 2; ■ 1.0% vol/vol, ■ 2.5% vol/vol, ■ 5.0% vol/vol, ■ 7.5% vol/vol, ■ 10.0% vol/vol) obtained with: (A) unmodified media, (B) 5.0 kDa MW mPEG PEGylated media, and (C) 20.7 kDa MW mPEG PEGylated media.

Note that the lefthand axis shows UV absorbance at 280 nm on a logarithmic scale to emphasize the retained contaminant peaks. The contaminant peak groups have been labelled as 1, 2, 3, and 4 as in Figure 3; the IgG elution peak has also been labelled. The steps in the chromatography protocol (bind/wash, elute/regenerate, and re-equilibrate) can be clearly identified by the mobile phase conductivity conductivity trace (dashed line) corresponding to the right axis of the graphs.

IgG recoveries achieved in the PEGylated columns were consistently and unexpectedly larger than those for the unmodified control columns. On average, for the IgG–YE mixtures, IgG recovery yields increased from $83.2 \pm 2.5\%$ in the unmodified columns to $91.9 \pm 2.1\%$ and $98.4 \pm 2.0\%$ in the 5.0 and 20.7 kDa PEGylated columns, respectively. In the case of the IgG–FBS mixtures, the average IgG recovery was $95.2 \pm 1.9\%$ in the unmodified column while the 5.0 and 20.7 kDa PEGylated columns had recoveries of $96.1 \pm 3.1\%$ and $98.1 \pm 1.8\%$, respectively. It should be noted also that the average IgG recovery percentages in runs without contaminants were $92.8 \pm 1.3\%$ in the unmodified column, $95.5 \pm 0.9\%$ in the 5.0 kDa PEGylated column, and $96.4 \pm 1.7\%$ in the 20.7 kDa PEGylated column.

The recovered masses of IgG and contaminants in each chromatogram of the spiking study were used to compute the corresponding selectivities under loading conditions. An application of Eq. (1) to our chromatograms suggests the definition of an operational selectivity as

$$\alpha_{\text{target,cont}} = \frac{m_{\text{IgG}}}{\left(m_{\text{cont,2}} + m_{\text{cont,3}} + m_{\text{cont,4}}\right)} \frac{m_{\text{cont,1}}}{\left(m_{\text{IgG,o}} - m_{\text{IgG}}\right)} \qquad (7)$$

where $m_{\text{IgG,o}}$ and m_{IgG} are the masses of IgG injected and recovered and $m_{\text{cont,i}}$ is the mass of contaminant species in peak group i. The selectivities computed with Eq. (7) are also plotted vs. contaminant spike concentration in Figure 10. In all cases, the PEGylated media had greater selectivities than the unmodified media, owing to the simultaneous

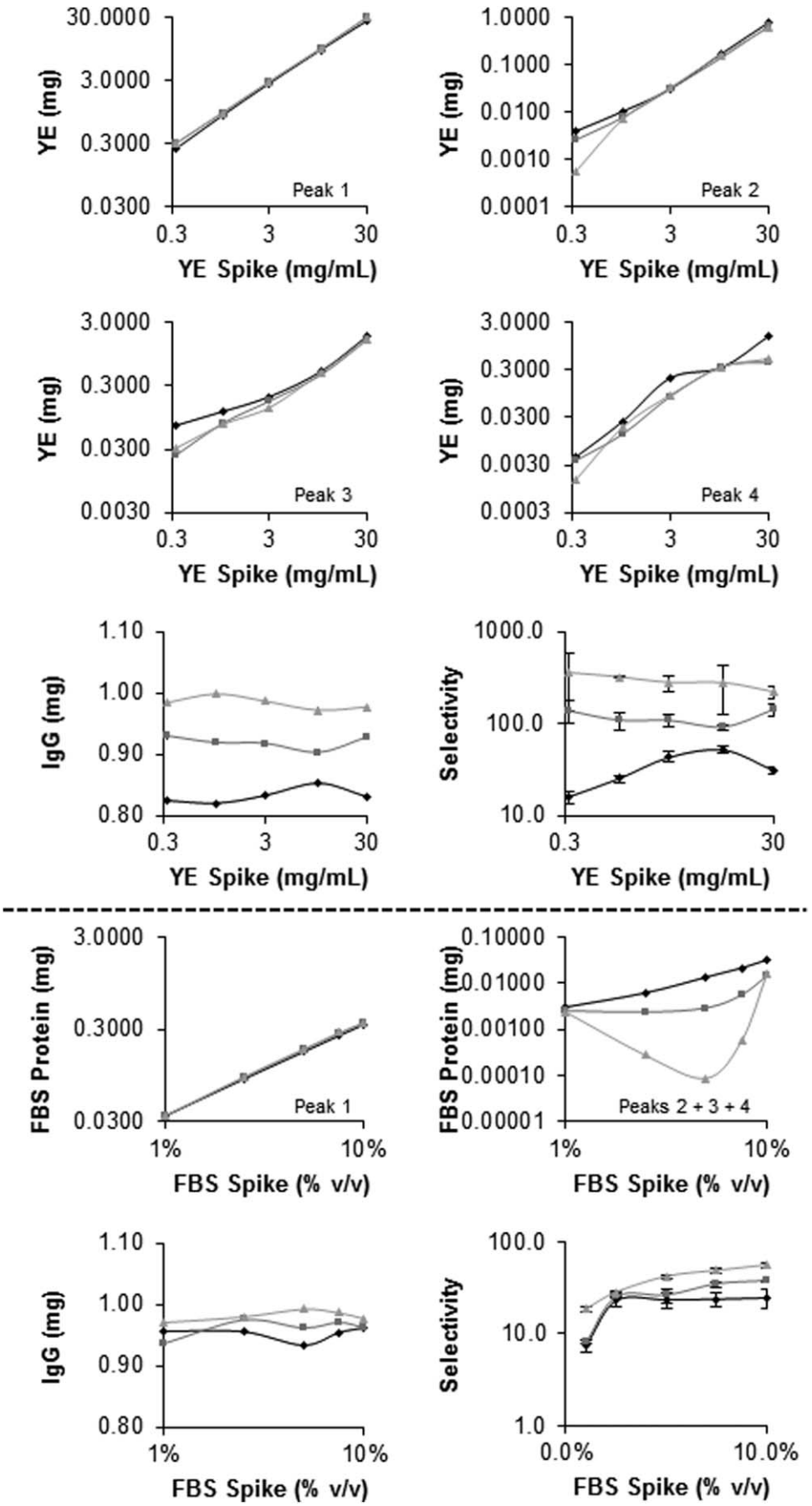

Figure 10. Mass recoveries of product and contaminant from the contaminant spiking studies of Figure 9.

The top plots correspond to the YE spiking study; the bottom plots to the FBS spiking study. The operational selectivities defined by Eq. (7) are also shown for each study. Symbols: unmodified commercial rSPA column (■), 5.0 kDa mPEG-rSPA column (■), and 20.0 kDa mPEG-rSPA column (■). Peak identities as in Figure 9. Error bars give the standard error of tripicate determinations.

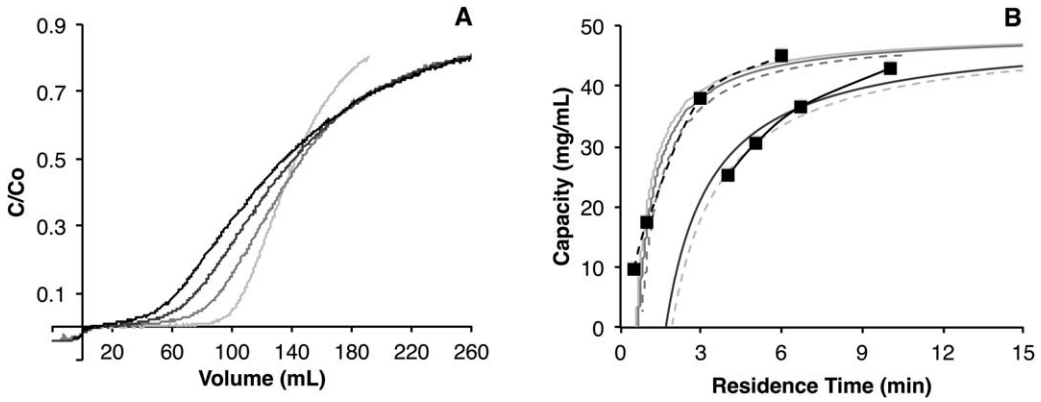

Figure 11. DBC determination for the 20.7 kDa PEG-rSPA column.

A: Breakthrough curves for 2 mg/mL IgG in pH 7 loading buffer as a function of flowrate, 0.50 (■), 0.75 (■), 1.00 (■), and 1.25 (■) mL/min. B: Experimental DBC determined at 10% breakthrough for the 20.7 kDa PEG-rSPA column (■) and the unmodified column (■, dashed). Un-modified column data was obtained from RepliGen product literature. Model dynamic capacity predictions shown with smooth curves. Pore diffusion-limited model predictions for the unmodified media are shown as (■) and modified media are shown as (■) using the corresponding IgG effective pore diffusisivities from Table 1. A pore diffusion-limited model prediction with the effective IgG pore diffusivity set to 2.2×10^{-8} cm^2/s is shown as (■). Combined pore diffusion and binding kinetics-limited model predictions shown for the modified media using the effective IgG pore diffusivity determined for the modified media and a kinetic on-rate constant of 10^5 $M^{-1}s^{-1}$ as (■, dashed) and 10^2 $M^{-1}s^{-1}$ as (■, dashed).

Table 1. Physical Characteristics of Base Matrix, Unmodified and PEGylated Chromatography Columns Used

Column	ε	β	β_{calc}	r_{pore} (nm)	D_e (cm^2/s) $\times$ 10^8	ψ	τ
Sepharose 4FF	0.341 ± 0.001	0.857 ± 0.002	N.A.	45.5 ± 0.5	7.3 ± 0.2	0.490 ± 0.002	2.1 ± 0.1
CaptivA PriMAB	0.374 ± 0.001	0.829 ± 0.003	0.84	50.1 ± 0.7	6.5 ± 0.3	0.523 ± 0.003	2.4 ± 0.1
5.0 kDa PEG–rSPA	0.296 ± 0.002	0.797 ± 0.003	0.83, 0.82	43.9 ± 0.7	5.1 ± 0.2	0.476 ± 0.004	2.8 ± 0.1
20.7 kDa PEG–rSPA	0.371 ± 0.004	0.784 ± 0.003	0.80, 0.78	41.0 ± 0.6	5.8 ± 0.3	0.450 ± 0.004	2.3 ± 0.1

Values reported for interstitial porosity, ε, particle porosity, β, particle porosity calculated from excluded volume considerations, β_{calc}, effective pore radius, r_{pore}, effective IgG pore diffusivity, D_e, diffusive hindrance factor, ψ, and tortuosity, τ. All values reported as the mean of triplicate determinations with associated 95% confidence limits. The β_{calc} values for the PEG-conjugated media list those estimated assuming volume additivity for the protein and PEG portions of the conjugates first followed by those estimated with the model of Fee and van Alstine.[40]

reductions in contaminant species binding and increases in IgG recovery. For the YE spiking experiments, the 5.0 kDa PEG–rSPA media was about five to ten times more selective on average than the unmodified media and the 20.7 kDa PEG–rSPA media was about ten to thirty times more selective. Selectivity increases were smaller, yet still significant in the FBS spiking experiments. At higher FBS concentrations, the selectivity of the 5.0 kDa PEG–rSPA media was about 50% larger than that of the unmodified media; the selectivity of the 20.7 kDa PEG–rSPA media was two to three times larger across the span of FBS concentrations used.

PEG–rSPA media dynamic binding capacity

The 20.7 kDa PEG–rSPA column was subjected to further testing to evaluate the impact of PEGylation on mass-transfer behavior. Breakthrough experiments were performed to evaluate DBC as shown in Figure 11A. The breakthrough curves are asymmetric and sharpened considerably at the lowest flow rate. These breakthrough curves are similar to those for an earlier generation protein A media where the asymmetry was ascribed to slow pore diffusion.[39] The linear driving force model will give asymmetric breakthrough curves when the number of transfer units is less than 20.[31] The corresponding dynamic binding capacities at 10% breakthrough for the PEGylated media are compared to vendor data[21] for the unmodified media acquired under similar conditions in Figure 11B. The DBC of the PEGylated media is about 60–80% of that of the unmodified media over the overlapping residence time range of 3–6 min. DBC could be restored to unmodified media values by doubling the residence time, at the cost of halving the throughput. It is clear that PEGylation with 20.7 kDa PEG has increased the overall IgG mass-transfer resistance. An increase in diffusive mass-transfer resistance in the pores of the media due to steric hindrance from the conjugated PEG chains was thought to be responsible.

PEG–rSPA media physical characterization

To support a more detailed study of mass-transport resistances in the modified media and to assess the magnitude of the steric barriers associated with ligand PEGylation, the column interstitial and media particle porosities and the effective pore radii of the PEGylated media columns were determined as were those of the Sepharose 4FF base matrix and unmodified CaptivA PriMAB columns. The results of these characterizations are reported in Table 1. Values of the interstitial and particle porosities were determined by the elution behavior of lambda DNA and iSEC, respectively. The iSEC probe partitioning data and Eq. (3) fits are shown in Figure 12; the assumed cylindrical pore model provides a good fit to the data. The particle porosity decreases monotonically in the order base matrix > unmodified media > 5.0 kDa PEG–rSPA media > 20.7 kDa PEG–rSPA media as expected based on consideration of the volumes occupied by the rSPA and PEG macromolecules in the pores. The particle porosity of the unmodified media is in line with those determined by Hahn et al.[26] for several different commercial, agarose-based protein A media.

As a check on experimental consistency, particle porosities for the ligand-based media were also calculated from the experimentally determined particle porosity of the base matrix by subtracting the excluded volumes of the immobilized rSPA and PEG–rSPA, given the known immobilized rSPA concentration and the extents of PEGylation. The equivalent sphere excluded volume of rSPA was estimated from its hydrodynamic radius, 2.9 nm, which was itself estimated from a correlation with molecular weight.[31] For the attached PEG chains, excluded volumes were estimated from the viscosity radii, 1.8 nm and 3.6 nm for the 5.0 kDa and 20.7 kDa PEG chains, respectively, which had also been estimated from a molecular weight correlation.[29] Two approaches were used to calculate the excluded volumes of the attached PEG chains: the first assumed that the rSPA and attached PEG chains occupied separate domains,[21] giving additive excluded volumes for the conjugate; the second used a model developed by Fee and Van Alstine[40] which equated the surface area-to-volume ratio of a PEG–protein conjugate in solution to that of a PEG molecule of equivalent total molecular weight. The calculated particle porosities agree well with the experimental values indicating that the experimental measurements are self-consistent. The Fee and Van Alstine model was in closer agreement with the conjugated media results than the volume additivity model. While we note that the differences between the model predictions are slight, and that these geometric predictions are approximate, they do suggest that the PEG portion of the conjugates may be somewhat more expanded than a typical random coil.

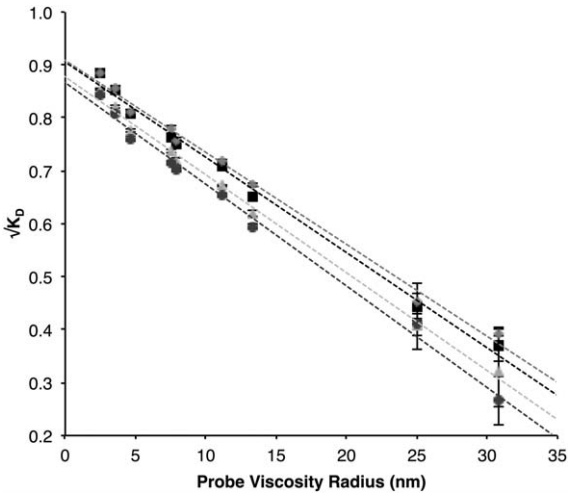

Figure 12. iSEC probe partition partitioning results.

Results plotted as the square root of the distribution coefficient vs. the viscosity radius of the probe species. Data shown for Sepharose 4FF (■), CaptivA PriMAB (◆), 5.0 kDa PEG-rSPA (▲), and 20.7 kDa PEG-rSPA columns (•). Lines represent weighted linear least squares fits to the data. Probe species comprised PEG, PEO, and dextran polymers. Error bars give 95% confidence limits of triplicate measurements.

The effective pore radius of the Sepharose 4FF base matrix determined by iSEC is in excellent agreement with that reported by Hagel et al.[41] The effective pore radius of the unmodified media was somewhat larger than that of the base matrix, perhaps reflecting repulsions between immobilized ligands or the response of the base matrix to the immobilization chemistry used. The effective pore radii of the PEGylated media were smaller than that of the unmodified media, as expected. The reduced particle porosities and effective pore radii further suggest that the diffusive mass-transfer resistance of the PEGylated media is elevated relative to the unmodified media.

PEG–rSPA media mass-transfer resistance analysis

A plate height analysis was mounted to further probe mass-transfer resistances in the base matrix, unmodified and PEGylated media columns. Representative IgG pulse response curves with and without the column under unretained conditions are shown in Figure 13A along with their corresponding exponentially modified Gaussian (EMG) function fits. The fitted peak moments, after correction for extra-column contributions, were used to estimate column plate heights as a function of mobile phase flow rate via Eq. (4). Dimensionless van Deemter plots were constructed by plotting the reduced plate heights vs. the reduced mobile phase velocities for each column and are shown in Figure 13B. Plate heights were found to range from tens of particle diameters to about one hundred particle diameters, consistent

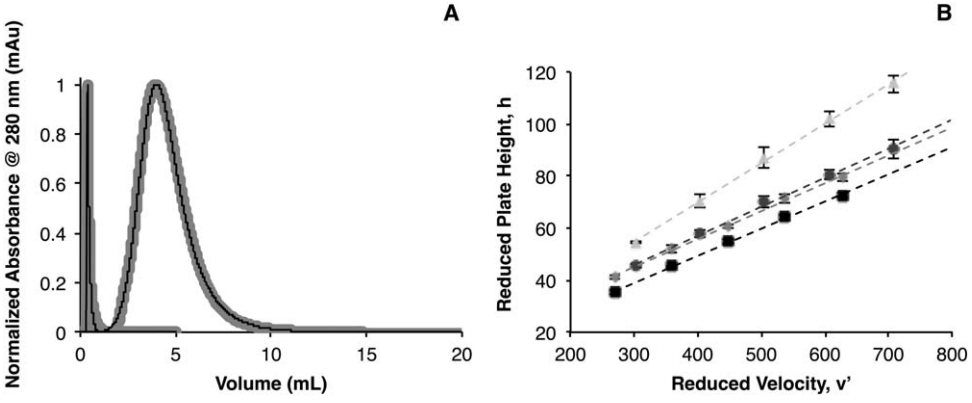

Figure 13. A: Representative pulse response data (thick gray lines) and EMG function fits (black lines) for the 20.7 kDa PEG-rSPA column.

The first peak is a column bypass response and the second is a corresponding inline column response. The flow rate was 1.0 mL/min and 100 μL of a 2 mg/mL IgG solution was injected in both cases. B: van Deemter plots of reduced plate heights, *h*, vs. reduced velocity, *v*, for Sepharose 4FF (■), CaptivA PriMAB (◆), 5.0 kDa PEG-rSPA (▲), and 20.7 kDa PEG-rSPA columns (•); extra-column band broadening and film mass-transfer contributions to plate heights have been subtracted. Symbols represent data derived from a moment analysis of the corresponding pulse response curves. Lines represent weighted linear least squares fits to the data. Error bars represent 95% confidence limits.

with the literature for other protein A-based media.[27] Equation (5) predicts a linear relationship between reduced plate height and reduced velocity and this is observed from the data. The fitted slopes provide estimates of the effective pore diffusivities of IgG in each media; these values are reported in Table 1. As expected, the pore diffusivities of IgG in each media are a factor of five to ten smaller than the bulk diffusivity and similar to those reported by others for IgGs in a variety of protein A media.[26,27,42] The effective pore diffusivity in the unmodified media was smaller than that in the base matrix and the effective diffusivities in the PEGylated media were smaller than that of the unmodified media.

Given the estimated bulk diffusivity of IgG and the particle porosities and effective pore radii of each media, the corresponding tortuosities, τ, of the pores could be estimated using[31]

$$D_e = \frac{\beta\psi D_o}{\tau} \tag{8}$$

where ψ is a hindrance factor accounting for molecular friction and wall interactions in confined pores. The value of ψ depends on the relative radii of the macromolecule and pore as[31,43]

$$\psi = 1 + \frac{9}{8}\lambda \ln \lambda - 1.539\,\lambda \tag{9}$$

where λ is the ratio of the molecular radius to the pore radius. Equation (9) is valid for $\lambda < 0.2$; using a Stokes–Einstein radius of $\sim$5 nm for antibody[31] together with our estimated effective pore radii, $\lambda \sim 0.1$ for all media examined here. Values for the hindrance factors and tortuosities are reported in Table 1. The computed tortuosities ranged from 2 to 3, consistent with literature values for Sepharose-based media.[44] While media with immobilized ligands all had tortuosities larger than that of the base matrix, the 5.0 kDa PEG–rSPA media had the largest tortuosity and that of the 20.7 kDa PEG–rSPA media was similar to that of the unmodified media.

With the effective IgG pore diffusivities now available, we revisited the DBC data of the 20.7 kDa PEG–rSPA media shown in Figure 11B and made predictions of DBC. We used the constant pattern solution to the general rate model by Hall[45,46] for simultaneous film and pore diffusion resistances to make these predictions without adjustable parameters. For an estimated ultimate DBC of 50 mg IgG/mL for the CaptivA PriMAB media, a pore diffusion and film mass transport-limited model with no fitted parameters reproduces the commercial media results very well as shown in Figure 11B. In this case, the number of transfer units associated with the film transport resistance is on the order of 300, while that associated with the pore diffusion resistance ranges from 10 to 20, depending on the liquid phase velocity. Unexpectedly, predictions using the same model with the reduced effective IgG pore diffusivity determined for the 20.7 kDa PEG–rSPA media did not describe the observed DBC of the modified media well: the effective pore diffusivity would have to be a factor of 2.5 times smaller than the experimental value in order to produce reasonable agreement. This suggests that there is an additional resistance that has not been taken into account.

We explored the possibility that there were simultaneous mass transfer and kinetic binding resistances by invoking the well-known Thomas[47] linear driving force solution of the general rate model as modified by Heister and Vermuelen[48] and systematized by Arnold and Blanch.[49] Using a value of 10^5 M^{-1} s^{-1} for the IgG–protein A media binding on-rate[31] and 2×10^6 M^{-1} for the equilibrium association constant[50] together with the determined effective pore diffusivity, we again predict the observed dynamic capacity of the unmodified media well. To mimic the dynamic capacity for the 20.7 kDa PEG–rSPA media, we must reduce the on-rate to order 100 M^{-1} s^{-1} when using the corresponding effective pore diffusivity of IgG. This is at the lower end of the on-rate range of 35 to 800 M^{-1} s^{-1} reported by Hahn et al.[9] for a number of different protein A media. This smaller binding on-rate used to mimic the observed dynamic capacity data for the PEGylated media gives the number of transfer units associated with kinetic resistances ranging from 2 to 6. The mobile steric barrier provided by the PEG chains attached to the ligand coupled with the confinement of the conjugate in the pore space may conspire to reduce the rate of productive binding collisions between the IgG and the immobilized rSPA ligand. This result is consistent with the work of Wen and Niemeyer[12] who studied the impact of PEGylation on the stability of an immobilized concanavalin A media and found a small reduction of the binding capacity and a lower adsorption rate of glucose oxidase on ligand PEGylation. While reduced pore diffusion accompanies ligand PEGylation, an unexpected significant increase the kinetic binding resistance may be the more important determinant of DBC.

Conclusions

We have shown that significant non-specific contaminant binding occurs in immobilized rSPA media and that it may be attributed to the immobilized ligand itself. A steric exclusion barrier in the form of ligand-conjugated PEG chains was introduced to reduce this non-specific binding to rSPA. Studies of IgG binding to immobilized and PEGylated rSPA on both analytical biosensor and chromatographic platforms indicated that the binding affinity for the target species could be maintained after PEGylation. We found that PEGylation enhanced the ability of rSPA media to reject the non-specific binding of YE and FBS components. The amount of non-specifically bound YE species was reduced on average by a third, from $\sim$15% to $\sim$9.5% retention for both modified columns over the range of concentrations studied; the FBS species binding nearly halved, from $\sim$5% retention to $\sim$3% retention. The modified media also provided small, but significant, increases of up to 15% in IgG recoveries on elution relative to the unmodified media. The combined reduction in contaminant binding and increase in IgG recovery led to average selectivity increases of over an order of magnitude in the YE spiking studies relative to the unmodified media. Selectivity increases in the FBS spiking studies were a more modest factor of two to three. The DBC of the PEGylated media was, however, reduced relative to the unmodified media and these reductions were attributed to decreased effective pore diffusivities and possible decreased ligand binding rates.

The PEGylation of macromolecular affinity ligands to improve selectivity by reducing non-specific binding is promising. While the absolute reductions in contaminant masses in some of the retained contaminant peaks were modest, the amounts retained in these peaks were modest to begin with; the aim is to reduce already low levels of contamination to negligible levels. Further, there is room for improvement as neither the extent of PEGylation nor the

nature of the PEG chains used was optimized in this study. Our initial extent of media PEGylation was low, less than one PEG chain per immobilized rSPA ligand, in order to limit presumed adverse impacts on mass-transfer resistances. And, only 5.0 and 20.7 kDa linear PEGs were used. Our future work will examine increased extents of PEGylation of rSPA with a wider range of PEG chain lengths and morphologies and will explicitly examine the corresponding impact on IgG selectivity, binding affinity, DBC, and media robustness.

Acknowledgments

The authors would like to thank CONACyT (Grant 53654 and Joint Fellowship 212025) and the ITESM Research Chair (Grant CAT161) in Mexico, and the Departments of Biomedical Engineering and of Chemical Engineering at Carnegie Mellon University for support. This material is also based in part upon work supported by the US National Science Foundation under Grant Number CBET-1159886. Any opinions, findings, and conclusions or recommendations expressed in this material are those of the author(s) and do not necessarily reflect the views of the National Science Foundation. The authors would also like to thank RepliGen, Inc. for their donation of rSPA chromatography media and free ligand for our study and Dr. Reddy's Laboratory for their donation of the aldehyde-activated PEGs.

Literature Cited

1. Roque ACA, Lowe CR, Taipa MÂ. Antibodies and genetically engineered related molecules: production and purification. *Biotechnol Prog*. 2004;20:639–654.
2. Ghose S, Allen M, Hubbard B, Brooks C, Cramer SM. Antibody variable region interactions with Protein A: Implications for the development of generic purification processes. *Biotechnol Bioeng*. 2005;92:665–673.
3. Shukla A, Thommes J. Recent advances in large-scale production of monoclonal antibodies and related proteins. *Trends Biotechnol*. 2010;28:253–261.
4. Hjelm H, Hjelm K, Sjöquist J. "Protein A" from *Staphylococcus aureus*. XXIII. Its isolation by affinity chromatography and its use as an immunosorbent for isolation of immunoglobulins. *FEBS Lett*. 1972;28:73–76.
5. Shukla AA, Hinckley P. Host cell protein clearance during protein A chromatography: development of an improved column wash step. *Biotechnol Prog*. 2008;24:1115–1121.
6. Gagnon P. *Purification Tools for Monoclonal Antibodies*. Tucson: Validated Biosystems, Inc.; 1996.
7. Nogal B, Chhiba K, Emery JC. Select host cell proteins coelute with monoclonal antibodies in protein a chromatography. *Biotechnol Prog*. 2012;28:454–458.
8. Tarrant RDR, Velez-Suberbie ML, Tait AS, Smales CM, Bracewell DG. Host cell protein adsorption characteristics during protein a chromatography. *Biotechnol Prog*. 2012;28:1037–1044.
9. Hahn R, Schlegel R, Jungbauer A. Comparison of protein A affinity sorbents. *J Chromatogr B*. 2003;790:35–51.
10. Roque ACA, Silva CSO, Taipa MÂ. Affinity-based methodologies and ligands for antibody purification: advances and perspectives. *J Chromatogr A*. 2007;1160:44–55.
11. Veronese FM, Pasut G. PEGylation, successful approach to drug delivery. *Drug Discov Today*. 2005;10:1451–1458.
12. Wen Z, Niemeyer B. Preparation and characterization of PEGylated Concanavalin A for affinity chromatography with improved stability. *J Chromatogr B*. 2011;879:1732–1740.
13. Peyser JR. Nucleic acids encoding recombinant protein A. US Patent no. 7,691,698 B2; 2010.
14. Greenwald RB, Choe YH, McGuire J, Conover CD. Effective drug delivery by PEGylated drug conjugates. *Adv Drug Deliv Rev*. 2003;55:217–250.
15. Harris JM, Chess RB. Effect of PEGylation on pharmaceuticals. *Nat Rev Drug Discov*. 2003;2:214–221.
16. Roberts MJ, Bentley MD, Harris JM. Chemistry for peptide and protein PEGylation. *Adv Drug Deliv Rev*. 2002;54:459–476.
17. Jentoft N, Dearborn DG. Labeling of proteins by reductive methylation using sodium cyanoborohydride. *J Biol Chem*. 1979;254:4359–4365.
18. Kinstler O, Gabriel N, Farrar C, DePrince, R. N-terminally chemically modified protein compositions and methods. US Patent no. 5,824,*784 A;* 1998.
19. Cisneros-Ruiz M, Mayolo-Deloisa K, Przybycien TM, Rito-Palomares MA. Separation of PEGylated from unmodified ribonuclease A using sepharose media. *Sep Purif Technol*. 2009;65:105–109.
20. Daly SM, Przybycien TM, Tilton RD. Adsorption of poly(ethylene glycol)-modified lysozyme to silica. *Langmuir*. 2005;21:1328–1337.
21. Pai SS, Hammouda B, Hong K, Pozzo DC, Przybycien TM, Tilton RD. The conformation of the poly (ethylene glycol) chain in mono-PEGylated lysozyme and mono-PEGylated human growth hormone. *Bioconjugate Chem*. 2011;22:2317–2323.
22. Sreerama N, Woody R. Estimation of protein secondary structure from circular dichroism spectra: comparison of CONTIN, SELCON and CDSSTR methods with and expanded reference set. *Anal Biochem*. 2000;287:252–260.
23. Wilson J, Scott I, McMurry J. Optical biosensing: kinetics of Protein A—IgG binding using biolayer interferometry. *Biochem Mol Biol Educ*. 2010;38:400–407.
24. Tobias R, Kumaraswamy S. In: FortéBio PC, editor. *Biomolecular Binding Kinetics Assays on the Octet Platform*, Vol. AN-14. United States: FortéBio, Pall Corporation; 2013:19.
25. Gong XW, Wei DZ, He ML, Xiong YC. Discarded free PEG-based assay for obtaining the modification extent of pegylated proteins. *Talanta*. 2007;71:381–384.
26. Hahn R, Bauerhansl P, Shimahara K, Wizniewski C, Tscheliessnig A, Jungbauer A, Comparison of protein A affinity sorbents II. Mass transfer properties. *J Chromatogr A*. 2005;1093:98–110.
27. Perez-Almodovar EX, Carta G. IgG adsorption on a new protein A adsorbent based on macroporous hydrophilic polymers. *I. Adsorption equilibrium and kinetics. J Chromatogr A*. 2009;1216:8339–8347.
28. Striegel AM, Yau WW, Kirkland JJ, Bly, D. *Modern Size-Exclusion Liquid Chromatography: Practice of Gel Permeation and Gel Filtration Chromatography*, 2nd ed. Hoboken: Wiley; 2009:32–33.
29. Squire PG. Calculation of hydrodynamic parameters of random coil polymers from size exclusion chromatography and comparison with parameters by conventional methods. *J Chromatogr*. 1981;210:433–442.
30. Gao H, Stevenson PG, Gritti F, Guiochon G. Investigations on the calculation of the third moments of elution peaks. I: Composite signals generated by adding up a mathematical function and experimental noise. *J Chromatogr A*. 2012;1222:81–89.
31. Carta G, Jungbauer A. *Protein Chromatography: Process Development and Scale-Up*. Weinheim: Wiley-VCH Verlag Gmbh & Co. KGaA; 2001:23, 179, 243–244, 253.
32. Tyn MT, Gusek TW. Prediction of diffusion coefficients of proteins. *Biotechnol. Bioeng*. 1990;35:327–338.
33. LeVan MD, Carta G. In: Green DW, Perry RH, editors. *Perry's Chemical Engineers' Handbook, Section 16: Adsorption and Ion Exchange*, 8th ed. New York: McGraw-Hill; 2007:16–21, 16–44.
34. Braisted AC, Wells J. Minimizing a binding domain from protein A. *Proc Natl Acad Sci USA* 1996;93:5688–5692.
35. Sjöholm I. Protein A from *Staphylococcus aureus*. Spectropolarimetric and Spectrophotometric studies. *Eur J Biochem*. 1975;51:55–61.
36. Surolia A, Pain D, Islam Khan M. Protein A: nature's universal anti-antibody. *Trends Biochem Sci*. 1982;7:74–76.
37. Hober S, Nord K, Linhult M. Protein A chromatography for antibody purification. *J Chromatogr B*. 2007;848:40–47.
38. Moks T, Abrahmsén L, Nilsson B, Hellman U, Sjöquist J, Uhlén M. Staphylococcal protein A consists of five IgG-binding domains. *Eur J Biochem*. 1986;156:637–643.

39. Fahrner RL, Blank GS. Real-time monitoring of recombinant antibody breakthrough during Protein A affinity chromatography. *Biotechnol Appl Biochem*. 1999;29:109–112.
40. Fee CJ, Van Alstine JM. Prediction of the vscosity radius and the size exclusion chromatography behavior of PEGylated proteins. *Bioconjugate Chem*. 2004;15:1304–1313.
41. Hagel L, Ostberg M, Andersson T. Apparent pore size distributions of chromatography media. *J Chromatogr A*. 1996;743:33–42.
42. Ghose S, Hubbard B, Cramer SM. Binding capacity differences for antibodies and Fc-fusion proteins on protein A chromatographic materials. *Biotechnol Bioeng*. 2007;96:768–779.
43. Brenner H, Gaydos LJ. The constrained Brownian movement of spherical particles in cylindrical pores of comparable radius. *J Colloid Interface Sci*. 1977;58:312–356.
44. Natarajan V, Cramer S. A methodology for the characterization of ion-exchange resins. *Sep Sci Technol*. 2000;35:1719–1742.
45. Hall KR, Eagleton LC, Acrivos A, Vermeulen T. Pore- and solid-diffusion kinetics in fixed-bed adsorption under constant-pattern conditions. *I&EC Fundamentals*. 1966;5:212–223.
46. Arnold FH, Blanch HW, Wilke CR. Analysis of Affinity Separations I: Predicting the Performance of Affinity Adsorbers. *Chem. Eng. J*. 1985;30:B9–B23.
47. Thomas HC. Heterogeneous ion exchange in a flowing system. *J Am Chem Soc*. 1944;66:1664–1666.
48. Heister NK, Vermulen T. Saturation performance of ion-exchange and adsorption columns. *Chem Eng Prog*. 1952;49:505–516.
49. Arnold FH, Blanch HW. Analytical affinity chromatography. II. Rate theory and the measurement of biological binding kinetics. *J Chromatogr*. 1986;355:13–27.
50. McCue JT, Kemp G, Low D, Quinones-Garcia I. Evaluation of protein-A chromatography media. *J. Chromatogr. A*. 2003;989:139–153.

Manuscript received Sept. 19, 2014